3

Neural coding by electroencephalography (EEG)

Yuan Yang

DEPARTMENT OF PHYSICAL THERAPY AND HUMAN MOVEMENT SCIENCES, NORTHWESTERN UNIVERSITY FEINBERG SCHOOL OF MEDICINE, CHICAGO, IL, UNITED STATES

Chapter outline

Introduction

The brain is the commander of voluntary movement control. It generates the oscillatory neural activity at specific frequency bands traveling through the corticospinal tract to activate the musculoskeletal system for movement execution [1]. Neural oscillations at mu (8–13 Hz) and beta (15–35 Hz) bands measured around the sensorimotor cortex, known as cortical sensory–motor rhythms (CSMRs), are thought to be associated with voluntary control of movements [2]. The coupling between CSMR and muscle activities has been previously reported at these frequency bands, confirming the key functional role of CSMR in movement control [3,4]. Damage to the corticospinal tract following a brain or spinal injury can result in a decrease in the coupling between CSMR and muscle activities, and associated motor impairments, such as muscle weakness and loss of independent movement control [5,6]. However, the CSMR may be preserved at the sensorimotor cortex that allows the identification of motor intentions via measuring and decoding the CSMR [7].

Intelligent Biomechatronics in Neurorehabilitation. https://doi.org/10.1016/B978-0-12-814942-3.00003-9

Electroencephalography (EEG) is an electrophysiological monitoring technique that records the oscillatory cortical activity including the CSMR. By placing the electrodes on the scalp, the EEG measures cortical activity without surgery. Compared to other brain signal recording methods (e.g., functional MRI, electrocorticography, positron emission tomography), the advantages of EEG are that it is inexpensive, low-risk, and portable [8]. These advantages allow EEG to be an online monitoring method for daily use. However, due to the volume conduction through the scalp, skull, and other layers of the brain, EEGs recorded by a scalp sensor are a "blurred" copy of multisource activities, which increases the difficulty of EEG signal decoding. Advanced signal processing methods are required to address this challenge. Traditional signal processing methods such as independent component analysis [9] and common spatial pattern (CSP) filter [10,11] need a large number of EEG electrodes covering the whole scalp during the measurement for disentangling the mixed multisource signals. This whole-scalp recording reduces the feasibility of EEG in neuro-rehabilitation for daily use. Several novel signal processing methods have been recently proposed to improve EEG data analysis for accurate identification of motor intentions using only a few electrodes. These novel methods can be combined with various new EEG devices with very few electrodes, such as the Emotiv Epoc headset and LooxidVR package for daily use.

Novel signal processing methods for few EEG electrode-based neural decoding

Spatial filter for improving signal-to-noise ratio

EEG signals recorded at each time point can be considered as a spatial matrix corresponding to the spatial distribution of the electrodes. Spatial filters are typically required to improve the signal-to-noise ratio (SNR) of EEG by using either the neighborhood [12] or global information [11]. Spatial filters using global information, such as the CSP algorithm [13] and the common average reference (CAR) [14], typically require a whole-scalp recording with a large number of EEG electrodes. To reduce the number of electrodes, we recommend the use of local spatial filters such as bipolar derivation [15] and Laplacian derivation [16]. Recent studies have demonstrated that the combination of local spatial filters and time-frequency analysis algorithm for extracting CSMR patterns can yield better results and use less electrodes than using global spatial filters [16–19].

Bipolar derivation

Bipolar derivation can increase the SNR by reducing the common noise of both electrodes. Let D_1 and D_2 be the discriminative patterns (e.g., CSMR) of EEG signals at the two recording electrodes. Let N represent the mixture of common additive background

noise of these two electrodes. The signals X_1 and X_2 recorded at these two EEG electrodes can be expressed by the following additive model:

$$X_1 = D_1 + N,\ X_2 = D_2 + N$$

This additive model is based on a basic assumption that a scalp EEG is a linear combination of source components. Although this assumption may not exactly reflect the complex composition of neural responses (which is still under exploration) in the scalp EEG, it is typically used as an approximate model in practice for artifact reduction and source analysis. Based on this model, the spatially filtered EEG signal derived from these two electrodes is:

$$X_{BI} = X_1 - X_2 = D_1 - D_2$$

Thus, the bipolar derivation can remove the shared additive background noise between two "active" electrodes.

Laplacian derivation

Laplacian derivation is also a widely used local spatial filtering algorithm in EEG signal processing. The Laplacian value of each electrode is obtained by subtracting the mean activity at surrounding electrodes from the electrode of interest. Denote by X_{LAP} the Laplacian filtered EEG signal at electrode i, and S_i an index set of the four electrodes surrounding the i-th electrode. The Laplacian derivation is computed according to the following formula:

$$X_{LAP} = X_i - \frac{1}{4}\sum_j X_j \quad (j \in S_j)$$

Two different sets of four surrounding electrodes are commonly used: nearest-neighbor electrodes (the distance from each surrounding electrode j to the center i is $d_{ij} = 3$ cm) and next-nearest-neighbor electrodes ($d_{ij} = 6$ cm). The Laplacian derivation employing nearest-neighbor electrodes is called a small Laplacian, while the one using next-nearest-neighbor electrodes is named a large Laplacian. The characteristics of the Laplacian derivation are highly dependent on d_{ij}. Experiments show that the Laplacian derivation becomes more sensitive to the components with high spatial frequencies when d_{ij} increases [20]. Thus, the small Laplacian is often used to improve the SNR when the signal is highly localized and stable over time, while the large Laplacian is more suitable when the signal is more distributed and nonstationary. Compared to the CAR, the Laplacian derivation uses local instead of global information to obtain a reference-free EEG. This method can be used where there are limited electrodes available to record EEG data.

Subject-specific channel selection for individualized recording setup

Previous studies show that actual or imaginary movements of different body parts can cause a decrease of signal power in the CSMR, called event-related desynchronization

(ERD), at corresponding ''active'' cortical regions; meanwhile, a power increase in the CSMR, known as event-related synchronization (ERS), might be observed at other ''idling'' areas [21,22]. In practice, many researchers simply place electrodes at three key positions (C3, Cz, and C4 of 10–20 EEG recording system [23]) over the sensorimotor areas, which generally covers the "active" regions controlling the upper and lower limbs. However, the precise functional regions may vary from subject to subject. Especially after a brain injury, the functional regions in the brain may be reorganized [24]. To address this problem, Yang and colleagues recently proposed a method based on the discriminative powers of different regions of interest (ROIs) to identify the optimal ROIs in the scalp for placing EEG electrodes [25]. The ROIs can be defined using EEG electrode positions according to an extended 10–20 recording system [23]. Assuming that the task is to identify the movement intention of the upper limb (U) versus the lower limb (L) as a two-class problem, the discriminative power of each ROI can be estimated using the Fisher's type F-score [26]:

$$F = \frac{\|\vec{\mu}_U - \vec{\mu}_L\|_2}{tr(C_U) + tr(C_L)}$$

where C denotes the covariance matrix of the feature vector extracted at this ROI, $\vec{\mu}$ denotes the mean of the feature vector, $\|\cdot\|_2$ denotes the $L2$-norm (Euclidean norm), and tr$(\cdot)$ the trace of a matrix.

Given an n-dimensional feature vector, $v(k) = [v_1(k),\ v_2(k),\ \ldots,\ v_n(k)],\ k = 1,\ \ldots,\ K$, where K is the number of samples (trials) for one class (U or L). Thus, the mean of the feature vector for the class is $\vec{\mu} = [\mu_1, \mu_2, \ldots, \mu_n]$, where $\mu_1, \mu_2, \ldots, \mu_n$ are the mean values of $v_1(k), v_2(k), \ldots, v_n(k)$, respectively. We denote by ${\sigma_1}^2,\ {\sigma_2}^2, \ldots,\ {\sigma_n}^2$ the variances of $v_1(i)$, $v_2(i), \ldots, v_n(i)$, respectively. Then the trace of the covariance matrix for each class can be computed as:

$$tr(C) = \sum_{i=1}^{n} \sigma_i^2 = \sum_{i=1}^{n} \left(\frac{1}{K-1} \sum_{k=1}^{K} (v_i(k) - \mu_i)^2 \right) = \frac{1}{K-1} \sum_{k=1}^{K} \left(\sum_{i=1}^{n} (v_i(k) - \mu_i)^2 \right)$$
$$= \frac{1}{K-1} \sum_{k=1}^{K} \|\vec{v}(k) - \vec{\mu}\|_2^2$$

Thus, the trace of the covariance matrix for each class is the mean Euclidean distance between samples to the class center, which reflects intraclass spread.

The F-score uses the Euclidean distance between class centers, $\left\|\vec{\mu}_U - \vec{\mu}_L\right\|_2$ to estimate the difference between classes and employs the trace of the covariance matrix to evaluate the variance within each class. The F-score can be extended to multiclass cases using either a one-versus-rest (OVR) strategy [16] or pairwise strategy [13]. The optimal ROIs should be selected with a large F-score to maximize the difference between classes and minimize the variance within each class. We can normalize the F-score by its maximum value over all ROI to obtain a topography of the discriminative power for selecting the key ROIs. Fig. 3.1 show an example of the selected ROI in different

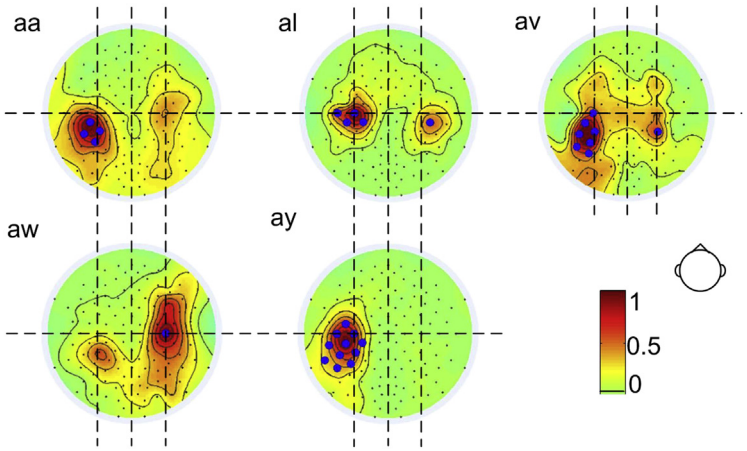

FIGURE 3.1 Selected ROIs (*blue dots* [black in print version]) in five different individuals for the identification of upper limb versus lower limb movement intentions. The *color bar* indicates the normalized *F*-score (range of value is between 0 and 1). The *dashed line* indicates the grid for defining the positions of Cz (middle cross), C3 (left cross), and C4 (right cross) in the 10–20 system. *Reproduced from YangY, Bloch I, Chevallier S, Wiart J. Subject-specific channel selection using time information for motor imagery brain–computer interfaces. Cognitive Computation 2016;8(3):505–518.*

individuals for the identification of upper limb versus lower limb movement intentions [26]. We can see that the selected regions could be different from subject to subject, indicating that a personalized setup is necessary for EEG recording based on few electrodes.

Time–frequency analysis for extracting CSMR

After placing the EEG electrodes on the optimal ROIs, the time–frequency analysis is required to extract the most discriminative CSMR patterns, since they are typically short-lasting (e.g., half to a few seconds depending on the movement duration) with the frequency range varying between subjects. Thus, a subject-specific time–frequency parameterization is required for CSMR pattern extraction. Various approaches have been previously proposed for this purpose [16,17,26–32]. Among the existing methods, the approach developed by Yang and colleagues yielded the best performance [16,17]. This time–frequency analysis approach is also based on the *F*-score and can be applied to both two-class and multiclass cases.

In this approach, the EEG signal at each electrode is decomposed into components in a series of overlapping time–frequency bins (ω_m, τ_n), $m \in \{1, 2, \ldots, M\}$, $n \in \{1, 2, \ldots, N\}$ with different frequency bands $\omega_m = [f_m, f_m + F - 1]$, $f_{m+1} = f_m + F_s$ (F is the bandwidth, F_s is the frequency step), and time intervals $\tau_n = [t_n, t_n + T - 1]$, $t_{m+1} = t_m + T_s$ (T is the interval width, T_s is the time step). The goal is to find a time–frequency bin that contains the most discriminative CSMR patterns for identifying the movement intentions.

Table 3.1 Comparison of using Yang's method and other methods on BCI competition IV dataset IIb for the identification of right versus left hand.

	Subject ID									
	1	**2**	**3**	**4**	**5**	**6**	**7**	**8**	**9**	**Mean**
Yang's method	0.39	**0.25**	0.13	0.93	**0.88**	**0.63**	0.55	**0.88**	**0.78**	**0.60**
FBCSP	0.40	0.21	**0.22**	**0.95**	0.86	0.61	0.56	0.85	0.74	**0.60**
CSSD	**0.43**	0.21	0.14	0.94	0.71	0.62	**0.61**	0.84	**0.78**	0.58
NTSPP	0.19	0.12	0.12	0.77	0.57	0.49	0.38	0.85	0.61	0.46

FBCSP, filter band CSP algorithm [34]; *CSSD*, common spatial subspace decomposition [35]; *NTSPP*, neural time series prediction preprocessing [36]. Yang's method yielded the best results on more subjects than the FBCSP, though their mean performances are the same. The best results are highlighted in bold.
Reproduced from Yang Y, Chevallier S, Wiart J, Bloch I. Time-frequency optimization for discrimination between imagination of right and left hand movements based on two bipolar electroencephalography channels. EURASIP Journal on Advances in Signal Processing 2014;2014(1):38.

We used the F-score to estimate the discriminative power of each time–frequency bin. The optimal time–frequency bin ($\omega^* \times \tau^*$) is found by exhaustively searching the largest F-score value among all regions:

$$F(\omega^*, \tau^*) = \max\{F(\omega_m, \tau_n) | m \in \{1,\ 2, \ldots, \mathrm{M}\}, n \in \{1,\ 2, \ldots, \mathrm{N}\}\}$$

Then, the CSMR patterns can be extracted from the optimal time–frequency bin by computing the variance of the ω^* band-pass filtered signal at the time segment defined by τ_n [17].

Tables 3.1 and 3.2 present a comparison using Yang's approach and other methods on two open-access EEG datasets for identifying movement intentions. The results are given in kappa coefficient [33]:

$$\kappa = (\mathrm{Acc} - \mathrm{Pe})/(1 - \mathrm{Pe})$$

where Pe is the chance level for agreement (i.e., $\mathrm{Pe} = 1/\mathrm{n}$ for n-class problems). Thus, a larger κ value indicates a better identification performance.

Table 3.2 Comparison of using Yang's method and other methods on BCI competition III dataset IIIa [37] for the identification of intentions of right hand, left hand, both feet, and tongue movement.

	Subject ID			
	1	**2**	**3**	**Mean**
Yang's method	0.64	**0.71**	**0.72**	**0.69**
AAR	0.70	0.37	0.39	0.49
ICA + PCA	**0.95**	0.41	0.52	0.63
JAD-CSP	0.76	0.41	0.53	0.57

AAR, adaptive autoregressive method [37]; *ICA + PCA*, combined method based on ICA and principal component analysis [38]; *JAD-CSP*, joint approximate diagonalization-based CSP [39]. The best results are highlighted in bold.
Reproduced from Yang Y, Chevallier S, Wiart J, Bloch I, Subject-specific time-frequency selection for multi-class motor imagery-based BCIs using few Laplacian EEG channels. Biomedical Signal Processing and Control 2017;38:302–311.

Remaining challenges and future directions

The state-of-the-art EEG signal processing methods allow the use of a small number of electrodes to identify movement intentions. However, the identification accuracy is still a challenge for reliable control of assistive devices (e.g., an electrical wheelchair) and neuro-prostheses. More advanced methods such as deep learning may be required to improve the identification accuracy in neural decoding using EEG. Meanwhile, other physiological signals such as electromyography and electro-oculography can also be used to realize a hybrid control [40–42], since these signals generally have a better SNR than EEG.

Traditional EEG sensors are "wet" electrodes that need a conductive gel applied to reduce the skin–electrode impedance. The user experience can be further improved by using a dry electrode. Although dry electrodes are now produced by several hardware producers, the quality of the signal might not be as good as with traditional "wet" electrodes. Most proposed EEG signal processing methods were tested on data recorded with "wet" electrodes. In the future, they should be further tested on data recorded using dry electrodes.

Despite the remaining challenges, EEG is still a promising technique for decoding movement intentions for helping individuals suffering from movement disabilities. EEG-based human–machine interfaces have the potential to become a next-generation intelligent biomechatronic technique for neurorehabilitation.

References

[1] Negro F, Farina D. Linear transmission of cortical oscillations to the neural drive to muscles is mediated by common projections to populations of motoneurons in humans. The Journal of Physiology 2011;589(3):629–37.

[2] McFarland DJ, Miner LA, Vaughan TM, Wolpaw JR. Mu and beta rhythm topographies during motor imagery and actual movements. Brain Topography 2000;12(3):177–86.

[3] Mehrkanoon S, Breakspear M, Boonstra TW. The reorganization of corticomuscular coherence during a transition between sensorimotor states. NeuroImage 2014;100:692–702.

[4] Yang Y, Dewald JP, van der Helm FC, Schouten AC. Unveiling neural coupling within the sensorimotor system: directionality and nonlinearity. European Journal of Neuroscience 2018;48(7):2407–15.

[5] Fang Y, et al. Functional corticomuscular connection during reaching is weakened following stroke. Clinical Neurophysiology 2009;120(5):994–1002.

[6] Rossiter HE, et al. Changes in the location of cortico-muscular coherence following stroke. NeuroImage: Clinical 2013;2:50–5.

[7] Shahid S, Sinha RK, Prasad G. Mu and beta rhythm modulations in motor imagery related post-stroke EEG: a study under BCI framework for post-stroke rehabilitation. BMC Neuroscience 2010;11(1):P127.

[8] Yang Y, Wiart J, Bloch I. Towards next generation human–computer interaction—brain–computer interfaces: applications and challenges. In: The first international symposium of Chinese CHI (Chinese CHI 2013); 2013. p. 1.

[9] Kachenoura A, Albera L, Senhadji L, Comon P. ICA: a potential tool for BCI systems. IEEE Signal Processing Magazine 2008;25(1):57−68.

[10] Ramoser H, Muller-Gerking J, Pfurtscheller G. Optimal spatial filtering of single trial EEG during imagined hand movement. IEEE Transactions on Rehabilitation Engineering 2000;8(4):441−6.

[11] Müller-Gerking J, Pfurtscheller G, Flyvbjerg H. Designing optimal spatial filters for single-trial EEG classification in a movement task. Clinical Neurophysiology 1999;110(5):787−98.

[12] Lou B, Hong B, Gao X, Gao S. Bipolar electrode selection for a motor imagery based brain−computer interface. Journal of Neural Engineering 2008;5(3):342.

[13] Yang Y, Chevallier S, Wiart J, Bloch I. Automatic selection of the number of spatial filters for motor-imagery BCI. In: The proceedings of the 20th European symposium on artificial Neural networks, computational Intelligence and Machine Learning (ESANN 2012); 2012. p. 109−14.

[14] Kübler A, et al. Patients with ALS can use sensorimotor rhythms to operate a brain−computer interface. Neurology 2005;64(10):1775−7.

[15] Yang Y, Chevallier S, Wiart J, Bloch I. Time-frequency selection in two bipolar channels for improving the classification of motor imagery EEG. In: The proceedings of the 34th annual international conference of the IEEE Engineering in medicine and biology society (EMBC'12); 2012. p. 2744−7.

[16] Yang Y, Chevallier S, Wiart J, Bloch I. Subject-specific time-frequency selection for multi-class motor imagery-based BCIs using few Laplacian EEG channels. Biomedical Signal Processing and Control 2017;38:302−11.

[17] Yang Y, Chevallier S, Wiart J, Bloch I. Time-frequency optimization for discrimination between imagination of right and left hand movements based on two bipolar electroencephalography channels. EURASIP Journal on Applied Signal Processing 2014;2014(1):38.

[18] Pfurtscheller G, Müller-Putz GR, Pfurtscheller J, Rupp R. EEG-based asynchronous BCI controls functional electrical stimulation in a tetraplegic patient. EURASIP Journal on Applied Signal Processing 2005;2005:3152−5.

[19] Kyrgyzov O, Bloch I, Yang Y, Wiart J, Souloumiac A. Data ranking and clustering via normalized graph cut based on asymmetric affinity. In: International conference on Image Analysis and Processing. Springer; 2013. p. 562−71.

[20] McFarland DJ, McCane LM, David SV, Wolpaw JR. Spatial filter selection for EEG-based communication. Electroencephalography and Clinical Neurophysiology 1997;103(3):386−94.

[21] Pfurtscheller G, Brunner C, Schlögl A, Da Silva FL. Mu rhythm (de)synchronization and EEG single-trial classification of different motor imagery tasks. NeuroImage 2006;31(1):153−9.

[22] Neuper C, Wörtz M, Pfurtscheller G. ERD/ERS patterns reflecting sensorimotor activation and deactivation. Progress in Brain Research 2006;159:211−22.

[23] Homan RW, Herman J, Purdy P. Cerebral location of international 10−20 system electrode placement. Electroencephalography and Clinical Neurophysiology 1987;66(4):376−82.

[24] Filatova OG, et al. Dynamic information flow based on EEG and diffusion MRI in stroke: a proof-of-principle study. Frontiers in Neural Circuits 2018;12.

[25] Yang Y, Kyrgyzov O, Wiart J, Bloch I. Subject-specific channel selection for classification of motor imagery electroencephalographic data. In: Acoustics, speech and signal processing (ICASSP), 2013 IEEE international conference on. IEEE; 2013. p. 1277−80.

[26] Yang Y, Bloch I, Chevallier S, Wiart J. Subject-specific channel selection using time information for motor imagery brain−computer interfaces. Cognitive Computation 2016;8(3):505−18.

[27] Bostanov V. BCI competition 2003-data sets Ib and IIb: feature extraction from event-related brain potentials with the continuous wavelet transform and the t-value scalogram. IEEE Transactions on Biomedical Engineering 2004;51(6):1057−61.

[28] Deng J, Yao J, Dewald JP. Classification of the intention to generate a shoulder versus elbow torque by means of a time−frequency synthesized spatial patterns BCI algorithm. Journal of Neural Engineering 2005;2(4):131.

[29] Luo T-j, Chao F. Exploring spatial-frequency-sequential relationships for motor imagery classification with recurrent neural network. BMC Bioinformatics 2018;19(1):344.

[30] Wang T, Deng J, He B. Classifying EEG-based motor imagery tasks by means of time−frequency synthesized spatial patterns. Clinical Neurophysiology 2004;115(12):2744−53.

[31] Yamawaki N, Wilke C, Liu Z, He B. An enhanced time-frequency-spatial approach for motor imagery classification. IEEE Transactions on Neural Systems and Rehabilitation Engineering 2006; 14(2):250−4.

[32] Gursel Ozmen N, Gumusel L, Yang Y. A biologically inspired approach to frequency domain feature extraction for EEG classification. Computational and Mathematical Methods in Medicine 2018; 2018:9890132.

[33] Carletta J. Assessing agreement on classification tasks: the kappa statistic. Computational Linguistics 1996;22(2):249−54.

[34] Ang KK, Chin ZY, Wang C, Guan C, Zhang H. Filter bank common spatial pattern algorithm on BCI competition IV datasets 2a and 2b. Frontiers in Neuroscience 2012;6:39.

[35] Wang Y, Zhang Z, Li Y, Gao X, Gao S, Yang F. BCI competition 2003-data set IV: an algorithm based on CSSD and FDA for classifying single-trial EEG. IEEE Transactions on Biomedical Engineering 2004;51(6):1081−6.

[36] Coyle D, McGinnity TM, Prasad G. Improving the separability of multiple EEG features for a BCI by neural-time-series-prediction-preprocessing. Biomedical Signal Processing and Control 2010;5(3): 196−204.

[37] Schlögl A, Lee F, Bischof H, Pfurtscheller G. Characterization of four-class motor imagery EEG data for the BCI-competition 2005. Journal of Neural Engineering 2005;2(4):L14.

[38] Blankertz B, et al. The BCI competition III: validating alternative approaches to actual BCI problems. IEEE Transactions on Neural Systems and Rehabilitation Engineering 2006;14(2):153−9.

[39] Grosse-Wentrup M, Buss M. Multiclass common spatial patterns and information theoretic feature extraction. IEEE Transactions on Biomedical Engineering 2008;55(8):1991−2000.

[40] Witkowski M, Cortese M, Cempini M, Mellinger J, Vitiello N, Soekadar SR. Enhancing brain-machine interface (BMI) control of a hand exoskeleton using electrooculography (EOG). Journal of Neuroengineering and Rehabilitation 2014;11(1):165.

[41] Yang Y, Chevallier S, Wiart J, Bloch I. A self-paced hybrid BCI based on EEG and EOG. In: 3rd workshop of tools for Brain-computer interaction (TOBI 2012); 2012. p. 42−3.

[42] Leeb R, Sagha H, Chavarriaga R, Millán J del R. A hybrid brain−computer interface based on the fusion of electroencephalographic and electromyographic activities. Journal of Neural Engineering 2011;8(2):025011.